

Investigation of stiffening scheme effectiveness towards buckling stability enhancement in tubular steel wind turbine towers

Nafsika Stavridou^{*1}, Evangelos Efthymiou^{1a},
Simos Gerasimidis^{1,2b} and Charalampos C. Baniotopoulos^{1,3c}

¹ Department of Civil Engineering, Aristotle University of Thessaloniki, Greece

² Department of Civil Engineering and Engineering Mechanics, Columbia University,
500 West 120th Street, NY 10027, New York, USA

³ School of Civil Engineering, University of Birmingham,
Edgbaston Birmingham, B152TT, United Kingdom

(Received August 27, 2014, Revised March 06, 2015, Accepted April 23 2015)

Abstract. Current climate conditions along with advances in technology make further design and verification methods for structural strength and reliability of wind turbine towers imperative. Along with the growing interest for “green” energy, the wind energy sector has been developed tremendously the past decades. To this end, the improvement of wind turbine towers in terms of structural detailing and performance result in more efficient, durable and robust structures that facilitate their wider application, thus leading to energy harvesting increase. The wind tower industry is set to expand to greater heights than before and tapered steel towers with a circular cross-section are widely used as more capable of carrying heavier loads. The present study focuses on the improvement of the structural response of steel wind turbine towers, by means of internal stiffening. A thorough investigation of the contribution of stiffening rings to the overall structural behavior of the tower is being carried out. These stiffening rings are placed along the tower height to reduce local buckling phenomena, thus increasing the buckling strength of steel wind energy towers and leading the structure to a behavior closer to the one provided by the beam theory. Additionally to ring stiffeners, vertical stiffening schemes are studied to eliminate the presence of short wavelength buckles due to bending. For the purposes of this research, finite element analysis is applied in order to describe and predict in an accurate way the structural response of a model tower stiffened by internal stiffeners. Moreover, a parametric study is being performed in order to investigate the effect of the stiffeners’ number to the functionality of the aforementioned stiffening systems and the improved structural behavior of the overall wind converter.

Keywords: wind turbine tower; stiffening ring; numerical analysis; shell elements; stringer stiffeners

*Corresponding author, Ph.D. Student, E-mail: nstavrid@civil.auth.gr

^a Lecturer, E-mail: vefth@civil.auth.gr

^b Ph.D., E-mail: sg2988@columbia.edu

^c Professor, E-mail: c.baniotopoulos@bham.ac.uk

1. Introduction

The use of alternative methods for energy production is considered crucial to maintain or improve the current climate conditions by reducing the emissions produced by the traditional energy production procedures. Wind energy as one of these alternative energy production methods is being developed rapidly during the past decades. In this paper, a new stiffening method is applied in order to improve the structural response of wind turbine towers. This stiffening method is trying to eliminate problems induced by local buckling phenomena, thus leading to safer and more robust structures, capable to maintain greater loads and achieving greater heights.

There are three types of steel wind turbine towers being nowadays constructed that vary by structural configuration/ morphology: a tapered tower, a jacket tower with a truss structure and a hybrid tower meaning a combination of a truss structure for the lower part and a tube for the upper one. Due to their advantages (easier mounting and structural detailing) tapered steel wind turbine towers are for the time being the most commonly used. They are composed of a number of steel tubular parts manufactured in the factory and mounted on site by means of bolted flanges. As the main supporting structure of a wind power plant is the tower, its structural analysis is considered important. The governing loads acting on the tower are the wind pressure up the height and the moment and lateral load generated by the rotor at the top of the structure. There have been several failures of wind turbine towers mainly due to extreme weather conditions, such as lightning or heavy storms and the most frequent failure mode for this type of long slender structures is local shell buckling (Lee and Bang 2013).

Steel tubular structures due to their geometry have the advantage of carrying great loads with small thicknesses allowing them to be widely applied in many branches of engineering and for that reason they have been thoroughly studied for more than one hundred years (e.g., Calladine 1989). Examples of their applications include silos, chimneys, nuclear reactors, pipelines etc. and recently wind turbine towers. Because of the thin wall of these structures in relation to the other dimensions, buckling is often the dominating failure mode. This is the reason why their buckling behavior has been thoroughly investigated in the past both experimentally and numerically with emphasis on the behavior of cylindrical shells. The behavior of cylindrical shells is practically the same with tapered towers since in the case of wind turbine towers the difference between the bottom diameter and the top diameter is trivial for the given distance between them, which leads the geometry of tapered towers to behave closer to cylinders than cones. There has been great scientific effort and work conducted by Timoshenko and Gere (1961), Bazant and Cedolin (2010), Vinson (1988), Galambos (1998), Teng and Rotter (2004) towards the interpretation and investigation of tubular structures. As stated by Teng (1996) the first shell buckling problem solved involved cylindrical shells under axial compression. From the very early experimental results driven by Flugge (1932) and Lundquist (1933), it was indicated that tubular structures buckle at loads significantly lower than the analytical predicted buckling load, which is the linear bifurcation load based on the assumptions of simple supports and a membrane state of pre-buckling stress distribution. Thorough research was conducted during the past decades on the investigation of this phenomenon. The discrepancy between experimental and theoretical results was attributed to initial geometrical imperfections, loading eccentricities, boundary conditions and differences in thicknesses and material properties. As the shell slenderness increases, the influence of those factors becomes more important (Dimopoulos and Gantes 2012).

The investigation of the structural behavior of wind turbine towers and their optimized response can result in more reliable and safer wind energy structures and subsequently, to more

efficient energy production. In particular, one of the main structural problems mentioned in wind energy structure reports is related to buckling phenomena of the wind turbine tower shell which led to a significant number of catastrophic accidents due to structural failure (Dimopoulos and Gantes 2013, Ragheb 2013, Lee and Bang 2013). The influence of the tower height to the failure of cylinders has been examined by Jansseune *et al.* (2012) and the response of cylindrical shells against wind loading and bending has been recently investigated by Chen *et al.* (2008) and Chen and Rotter (2012). As the most suitable load-carrying structure for a wind turbine is a steel tapered tower, composed of subsequent tapered shell members mounted on site (Bazeos *et al.* 2002), there have been several studies focusing on the structural behavior of these structures. Chen *et al.* (2011) performed a meticulous study to calculate the buckling performance of cylindrical shells with variable wall thickness. Lavassas *et al.* (2003) has modeled and analyzed a prototype 1 MW tapered steel wind turbine tower with emphasis on structural detailing of the rings, opening and foundation anchoring. Bazeos *et al.* (2002) conducted a stability analysis on a steel wind turbine tower with varying diameter and thickness along its height, resulting in useful results concerning the static and seismic response of the tower by comparing detailed and simplified models, while Lee and Bang (2013) have performed the numerical analysis of a collapsed wind turbine tower in Korea in 2005, achieving very good agreement between the analytical results of the shell FEM model and the measured results of the accident. Dimopoulos and Gantes (2012) have performed experiments and have elaborated numerical results on different types of stiffening around the openings of wind turbine towers achieving to counterbalance the loss of strength due to the opening with various alternative stiffening schemes. The results of the comparison between the experimental and numerical results showed that in shells without openings, the presence of initial imperfections plays a vital role in the numerical analysis and that the estimation of the initial imperfections shape can be fulfilled taking into account the shape of the first eigenmode. Experimental results of a full scale wind turbine monitoring research have been obtained giving detailed information on the loading conditions and response of connections and internal stiffeners throughout the structure's life (Rebello *et al.* 2012a, b). Arasu *et al.* (2011) successfully performed numerical analysis to assess the seismic response of steel wind turbine towers and a methodology is followed to investigate the probability of reaching certain damage levels and Nuta *et al.* (2011) outlined a methodology for seismic risk assessment of tubular steel wind turbine towers subjected to several levels of seismic hazard through the calculation of fragility curves. The optimal design of wind turbine towers and the optimal positioning of rings stiffeners towards the design of the most cost effective structures which are structurally safe has been the topic of research of Uys *et al.* (2007) while Negm and Maalawi (2000) elaborated several optimization strategies for structural optimization of wind turbine towers. Stavridou *et al.* (2013) performed numerical analysis on a wind turbine tower with and without stiffening rings confirming the beneficial effect of stiffening rings in the overall tower performance. Sandwich cylindrical shells due to their higher stiffness/weight and strength/weight ratios compared to conventional shells have wide applications and their buckling behavior is further investigated currently (Ohga *et al.* 2005). The issue of limiting shell buckling and further stiffening shells against local buckling by means of circular stiffeners that are placed at regular intervals along the cylinder has initially been introduced and examined by Rotter (1987) and further investigated by Schneider and Zahlten (2004), Schneider and Brede (2005) and Lemak and Studnicka (2005). Regulations for the design and positioning of stiffeners have been introduced in design recommendations in the European Recommendations by the European Convention For Constructional Steelwork (2008). Stringer stiffened cylindrical shells are more widely employed to counterbalance axial loads, bending moments and shear forces

and have thoroughly been examined by Singer (2004) and his scientific team. The longitudinal stiffeners serve mainly to increase the axial and bending strength of cylindrical shells, which has recently been verified by Arani *et al.* (2010). 3D finite element analyses conducted by Wojcik *et al.* (2011) have shown that the buckling strength of perfect cylindrical shells is three times higher than the ones that take into account initial imperfections, whereas material non-linearity significantly reduces their buckling strength.

Despite the great scientific progress carried out in the field of tubular structures, there is limited work devoted to the stiffening of wind turbine towers with internal rings and stringer stiffeners and the investigation of their effectiveness against buckling phenomena. In order to fulfill the needs of these tall and slender structures against combined loading, a numerical study is conducted in order to investigate the effect of internal stiffeners against local buckling and bending and thus improving the overall behavior of the structure. The numerical analyses are performed with the use of the commercial finite element program Abaqus (Documentation, Abaqus and User manual, 2012). From the structural point of view, the stiffening rings contribution to local buckling is highlighted and their number up the tower length is discussed. The longitudinal stiffeners play a vital role in the bending behavior of the structure and their optimal number and distribution around the circumference of the tower is discussed. The internal stiffeners are applied according to the relevant literature, and their theoretical benefit for slender structures is verified numerically through a parametric study. Linear perturbation analysis is performed for the unstiffened structure providing the first eigenmode shape which is used with the relevant imperfection factor as initial imperfections of the structure for the non-linear analysis. Multiple stiffening schemes with different number/locations of rings are in addition examined applying non-linear imperfection analysis techniques.

2. Buckling resistance of steel tubular structures

The study of cylindrical wind turbine towers lies in the field of cylindrical shells under combined loading of transverse and compressive loads and bending moment. They are considered thin-walled structures and their main use in everyday life is for the construction of chimneys, tanks, pipelines and silos and recently on wind turbine structures.

In long and slender steel cylindrical shells, large non-elastic deformations lead to buckling or plastic failure. Thin shells structures transfer loading by means of the membrane tensile and compressive forces that act in the walls of the shell. Their efficiency in load bearing capacity is rather high under symmetrical loading and boundary conditions, while a more complicated behavior is observed under asymmetrical loading or local load concentration.

As structures are becoming more and more complicated there have been more sophisticated methods for analyzing shell structures. Wind turbine towers have a similar function to chimneys as they are tall and slender steel tapered structures which can be designed according to regulations set in EN 1993-3-2 (2006). Very rarely these structures are designed like simple cantilevered structures without any more detailed finite element analysis. The formulae for first and second order beam theory provided in the above mentioned document can be applied only under circumstances when preliminary checks have to be conducted and future detailed analyses are to follow. It is common practice that more complicated and accurate analyses for these structures is performed like linear elastic, material non-linear, material and geometric non-linear, with or without imperfections methods of analysis which are available and are included in the new EN

1993-1-6 (2006) for the design of steel shell structures. When the computational capacity is limited, there can be a first approach to buckling problems of shells by conducting a linear elastic buckling analysis, to determine the bifurcation load of the perfect structure. The limitation of this approach is that the reduction factors applied to account for geometric imperfections and plasticity are difficult to determine. A fully nonlinear analysis with large deflections, geometric imperfections and plasticity among other difficulties involves the difficulty of establishing the shape and amplitude of initial imperfections for the analysis. Koiter (1945) first and Speicher and Saal (1991) some years after suggest that an equivalent imperfection of the same form as the first bifurcation mode with an adjusted amplitude is the safest way to introduce imperfections in the model.

The current work aims at investigating the stability capacity of cylindrical steel wind turbine towers and the contribution of internal stiffening schemes to that capacity. To investigate the contribution of the stiffening schemes to the overall behavior of a wind turbine tower, geometrical and material nonlinear analysis is applied as prescribed both for the ultimate limit state and the buckling limit state in the European Standard, (EN 1993-1-6 2006). Shell structures are very sensitive to the type of constraint conditions and for the case of wind turbine towers that are closed cylinders, both the top rigid plate carrying the mechanical equipment and the stiffening rings are considered pin ends and the foundation is considered clamped. In the same standard provisions for the implementation of stringer stiffeners are provided in order to increase the stability of the structure, assisting with the introduction of local loads along the meridian of the shell. These longitudinal stiffeners are considered to ensure the higher capacity of the structure towards shear, axial and bending loads and provisions for their application are prescribed in relevant Standards (EN 1993-1-6 2006 and DNV-RP-C202 2013). Stiffened towers demonstrate a deformed shape closer to the beam theory than unstiffened ones, which is also demonstrated also by the higher critical load of the stiffened structure compared to the unstiffened one.

3. Stiffening schemes: Role and characteristics

3.1 Stiffening rings

Stiffening rings are often an integral part of shell structures while their most common failure mode is the out-of-plane buckling (Bushnell 1976). The critical values for the capacity and the minimum thickness of the wall are calculated according to the length to diameter ratio and the appropriate factor of safety. In the case of long cylindrical shells stiffened by rings, provided that the rigidity of the rings is such that they are able to carry the lateral load without in-plane buckling of the rings, the critical buckling length is considered to be the distance between the rings.

The stiffening rings examined in the present study are local stiffening members that pass around the internal circumference of the shell revolution at a given point at the meridian. The cross section of these sub-structures may vary from single plated to "T" or "L" profiles, but the single plated are mostly used in the wind turbine tower stiffening due to simpler implementation and welding. Their potential out-of-plane deformation is limited with appropriate thickness used, whereas their in-plane stiffness is comparably high. The orientation of the rings and their specific dimensions are given in Fig. 1.

When designing wind turbine towers according to the European Standards (EN 1993-1-6 2006), there are four limit states that have to be taken into account: LS1-plastic limit state, LS2-cyclic

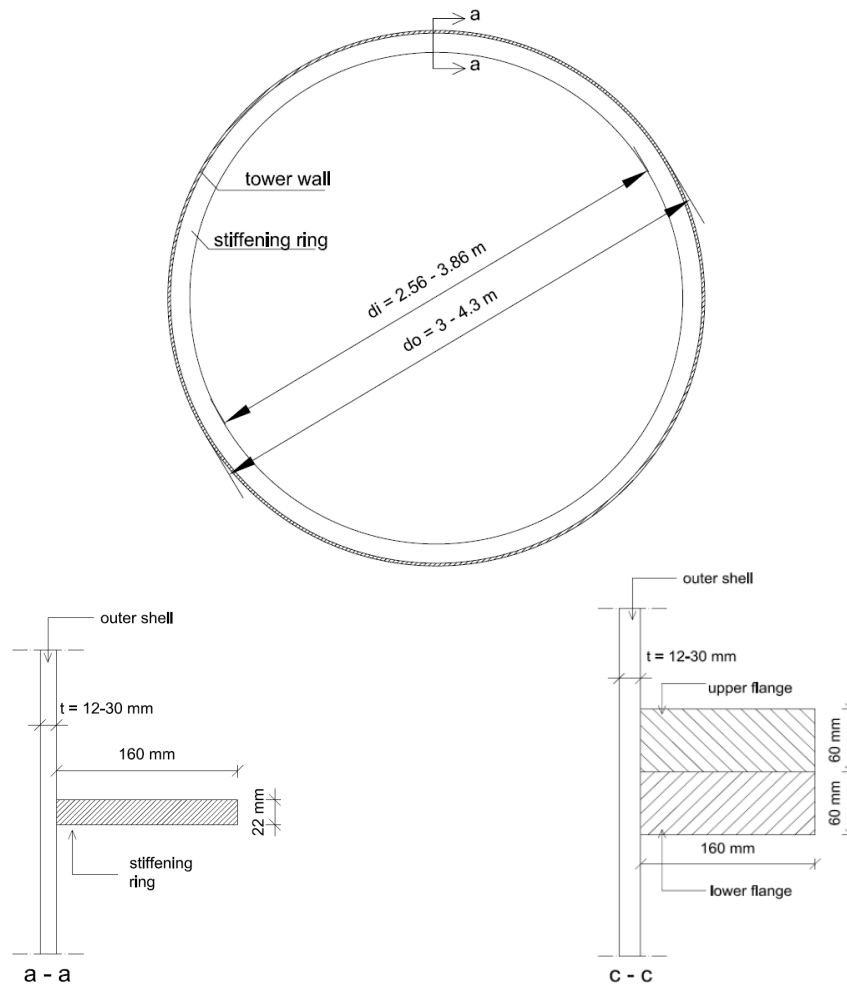


Fig. 1 Dimensions of stiffening rings and flanges

capacity, LS3-Buckling limit state and LS4-Fatigue limit state.

Since the beneficial influence of the stiffening rings is observed in the design according to the plastic limit state (LS1) and the buckling limit state (LS3), focus is given in the present paper on how the rings change the tower behavior towards the loading governing these limit states. No special reduction factors for lowering the buckling resistance of the shell due to welding of stiffeners are used in practice. The possible modification of the fatigue resistance of the tower shell can only be discussed in the Fatigue limit state which is out of the scope of the present paper. In the plastic limit state, the beneficial impact of the stiffening rings to the overall performance of the shell is mainly on the relief of the excessive strain concentration on the flanges due to the concentrated circumferential stresses.

In the analysis of the structure with the buckling limit state (LS3) loads, there are two factors that have to be taken into account. Firstly, the circumferential buckling strength of the shell is limited, due to the small thickness to radius ratio of the tower shell. Secondly, as described in analytical form in article 7.9 of Eurocode (EN 1991-1-4 2006), the wind force around the

circumference of the shell, tends to “ovalize” the circular cross-section, having as a result the presence of high circumferential stresses and second order effects (Stathopoulos and Baniotopoulos 2007).

The contribution of internal stiffening rings is considered beneficial, for all the above mentioned issues. The tower's buckling capacity is increased and the maximum concentrated circumferential stresses are noticeably reduced. There are various methods that can be followed to verify the structure towards local buckling specified in EN 1993-1-6 (2006).

The relief of the circumferential stresses due to the use of stiffening rings is verified analytically when examining the expression for the calculation of the critical circumferential buckling stress given in Annex D of (EN 1993-1-6 2006) where for long cylinders the critical circumferential buckling stress should be obtained from the following Eqs. (1)-(3). In this framework, for long cylinders

$$\frac{\omega}{C_\theta} > 1.63 \frac{r}{t} \quad (1)$$

the critical circumferential buckling stress is

$$\sigma_{\theta, Rcr} = E \left(\frac{t}{r} \right)^2 \left[0.275 + 2.03 \left(\frac{C_\theta}{\omega} \cdot \frac{r}{t} \right)^4 \right] \quad (2)$$

$$\omega = \frac{l}{\sqrt{r \cdot t}} \quad (3)$$

where: ω is the dimensionless length parameter, r the cylinder radius, t the shell thickness, l the cylinder length, C the external pressure buckling factors according to boundary conditions and E the Young's modulus of the material. Starting the solution from Eq. (3), where l is maximized for longer cylinders (where l is greater), it can be derived from Eq. (2) that for a given significant value of the length l between the boundaries, the critical circumferential buckling stress is minimized. The critical buckling length is considered the length between boundaries or built-in edges, having a smaller value for l when taking the distance between consequent stiffeners. The same relief of meridional buckling stresses is observed when examining the analytical equations given for the calculation of the critical meridional buckling stresses by the following expressions: the critical meridional buckling stress is

$$\sigma_{x, Rcr} = 0.605 E C_x \frac{t}{r} \quad (4)$$

Where C_x is calculated by Eq. (5)

$$C_x = 1 + \frac{0.2}{C_{xb}} \left[1 - 2\omega \frac{t}{r} \right] \quad (5)$$

where: t , l , r , E and ω are already defined. C_{xb} takes a different value according to the type of boundary condition at the ends of the reference shell part. For the critical meridional stress as well the smaller the distance between two ends, the critical stress is maximized.

The function of rings is focusing on limiting the out-of-roundness deformation of the cross-

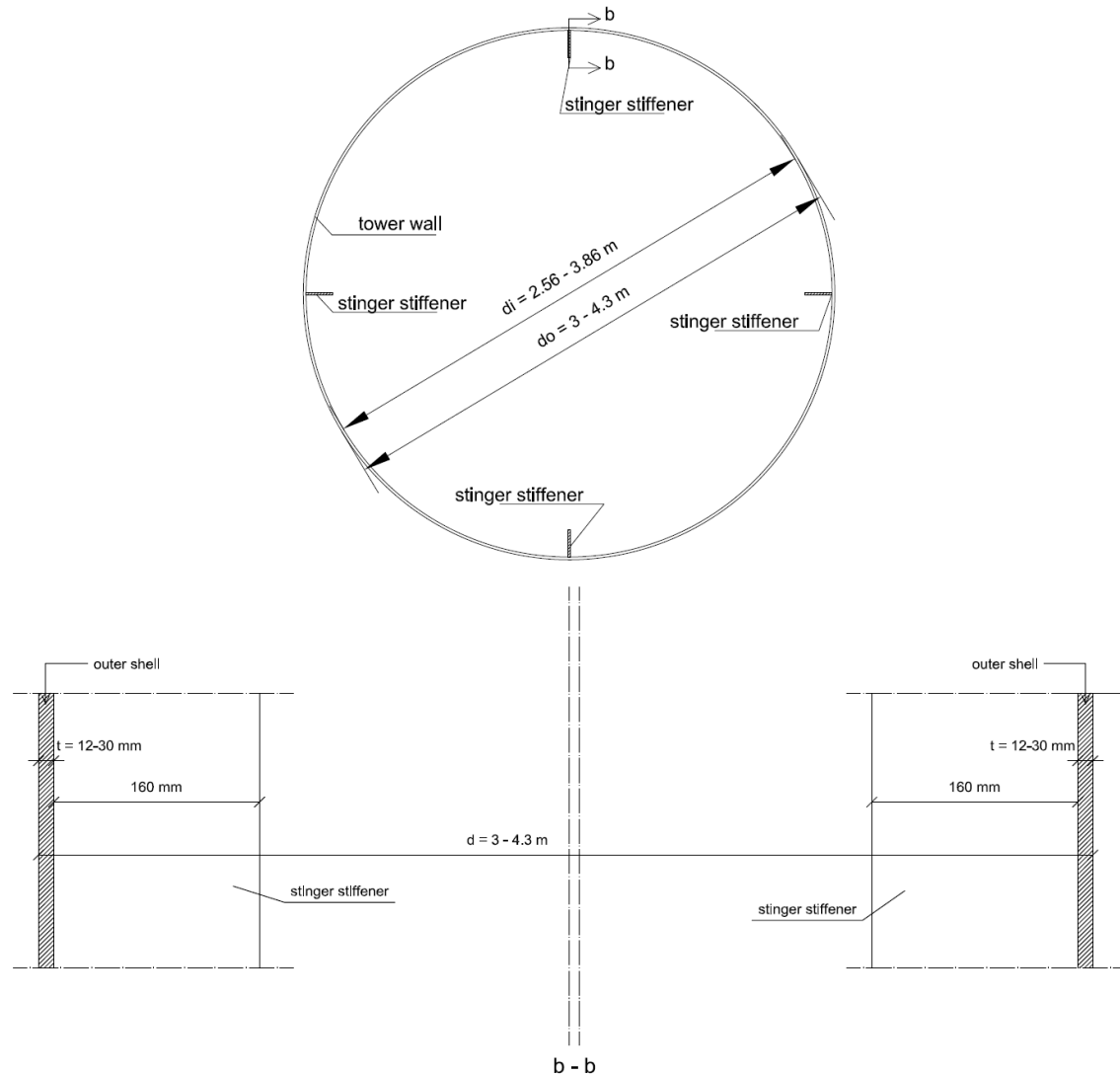


Fig. 2 Dimensions stringer stiffeners

section, eliminating “ovalization”, therefore the critical circumferential buckling stress is maximized when the distance between rings is minimized. Therefore, for achieving higher critical circumferential and meridional buckling stresses, the manufacturing of internal stiffening rings is strongly recommended.

3.2 Stringer stiffeners

Longitudinal stiffeners are the commonest stiffening type of shell structures. When designed properly providing sufficient stiffness to the shell and are widely spaced, the commonest failure mode is typical local shell buckling in the area between the stringers, and when they are closely spaced the most common failure mode is panel shell buckling, where the stiffeners deform along

with the outer shell generating a general instability failure (DNV-RP-C202 2013).

The stringer stiffeners implemented and presented in the present study are local stiffening members following the meridian of the shell and representing a generator of the shell of revolution. The cross section of these stiffening members is commonly single plated or of “T” profiles, and the single plated are mostly used in the wind turbine tower stiffening due to simpler implementation and welding. As discussed for the stiffening rings, the potential out-of-plane deformation of stinger stiffeners is limited with appropriate thickness used, whereas their in-plane stiffness is also comparably high. The position of the longitudinal stiffeners and their detailed dimensions are given in Fig. 2.

4. Numerical investigation of a wind turbine tower

4.1 Description of the structure

The wind turbine tower used for the implementation of stiffening rings has been examined in the HISTWIN project (Veljkovic *et al.* 2006) and has a hub height of 76.15 meters and due to elements’ transportation limitations, it consists of 3 parts that are mounted on site. These parts vary in length: 21.8 m, 26.6 m and 27.8 m from bottom to top. The tower is not cylindrical as the lower diameter of the tower is 4.3 m and the top one is 3 m. The thickness of the shell wall is also not constant, starting from 12 mm at the top to 30 mm at the bottom. The tower is embedded into a reinforced concrete foundation which is anchored to the ground and therefore the tower is considered to be fixed at the foundation which is not modeled. A boundary condition constraining all translational and rotational degrees of freedom is used to model the foundation of the structure.

4.2 Design loads

When designing wind turbine towers, the loads that the tower has to resist are:

- (1) the self-weight of the tower,
- (2) the forces acting on the tower due to the function of the nacelle provided by the manufacturer,
- (3) the fatigue loads that are again provided by the manufacturer,
- (4) possible icing around the shell of the tower and
- (5) the wind load that is distributed along the height of the tower.

The focus is oriented in analyzing the structure and examining the influence of the implementation of stiffening rings towards the complex loading condition of the tower.

4.3 Loads taken into account in the analysis

In the present work, the towers are supposed to operate in environments where the driving effect is extreme wind and not fatigue deriving from conventional operation of the wind turbine. The focus therefore is concentrated on the contribution of stiffening rings for improving the tower behavior against local buckling coming from extreme loading. Therefore the fatigue, the seismic and icing loading are not taken into account. The loads that are used in the analyses are characteristic loads provided by the manufacturer and refer to the maximum force imposed to the tower due to the operation of the mechanical system. Moreover, the weight of platforms and

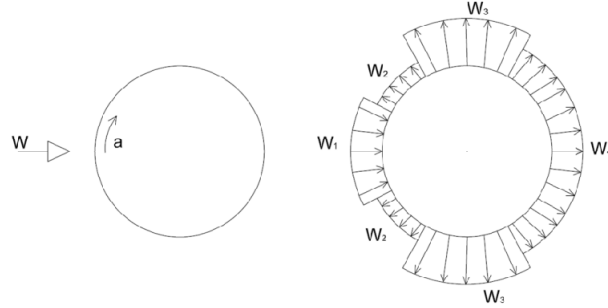


Fig. 3 Wind load distribution along the circumference of the tower

ancillary equipment of the tower is neglected. The self weight of the tower shell is automatically calculated by the FE software ABAQUS taking into account the dimensions of the tower and the material density. Wind loading is calculated according to the Eurocode (EN 1993-1-6 2006) as a complex function related to the Reynolds number of the wind flow and the position around the circumference. For the model described, the circumference of the shell is divided in 8 zones of homogenous pressure to simulate the wind loading given by the Eurocode diagram, as shown in Fig. 3.

The concentrated loads are applied at the top of the tower to a reference point taking into account the eccentricity of the rotor position, shown in detail in Fig. 4. The loading of the nacelle is provided by the producer and is as following: Total weight of nacelle, blades and rotor (R_V) is 1080 kN and is positioned at the top of the tower having the center of gravity shifted horizontally + 0.725 m from the axis of the tower and vertically + 0.50 m above the upper flange level (+76.15 m). According to manufacturer's data, the rotation of the blades is producing a concentrated horizontal force (R_H) of 600 kN at (76.15 + 0.5) m and a bending moment (R_M) of 48000 kNm at the same point. The loading condition of the tower is the combination of the loads described above

$$P = \{R_V + R_H + R_M\} + W \quad (6)$$

The loads over the tower stem are calculated, for the specific dynamic characteristics and geometry of the structure, according to Eurocode (EN 1991-1-4 2008). In the case under investigation, the basic wind velocity at 10m above the ground is taken as $v_b = 27,00$ m/sec and the terrain category is [II]. The distribution of the wind forces up the height $[z]$ of the shell is given as a function of the diameter $[D]$. The wind force F_w is given in kN/m. This wind is the extreme wind and is supposed to have a return period of 50 years.

$$\text{For } z \leq 2m : F_w = 0,51 \cdot D \quad (7)$$

$$\text{For } z > 2m : F_w = 0,013 \cdot \ln(20 \cdot z) \cdot [\ln(20 \cdot z) + 7] \cdot D \quad (8)$$

Where, $D = -0,01775 \cdot z + 4,30266$

The wind pressure according to Eqs. (7) and (8) that is applied on the surface of the tower is

$$\text{For } z \leq 2m : p_w = [0,51 \cdot D] / [\theta \cdot (D/2)] \quad (9)$$

$$\text{For } z > 2m : p_w = \{0,013 \cdot \ln(20 \cdot z) \cdot [\ln(20 \cdot z) + 7] \cdot D\} / [\theta \cdot (D/2)] \quad (10)$$

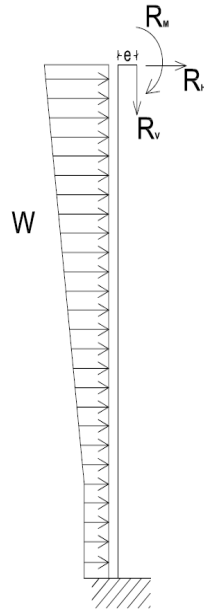


Fig. 4 The loads used for the analysis of the tower

And according to the Eurocode, the wind pressure around the circumference of a cylinder is non-uniform and is calculated taking into account the external pressure coefficient ($c_{p,0}$) without free-end flow and the end-effect factor $\phi_{\lambda\alpha}$ as shown in Eq. (11) below

$$w = c_{p,0} \cdot \phi_{\lambda\alpha} \cdot p_w \quad (11)$$

Taking into account the Eqs. (9), (10) and (11) along with Fig. 2 the wind pressure around the circumference and up the height of the cylindrical tower is given by the expressions

$$w = \begin{cases} w_1 = p_w & [0 \div 30^\circ] \\ w_2 = 0,6 \cdot p_w & [30^\circ \div 60^\circ] \\ w_3 = 1,85 \cdot p_w & [60^\circ \div 120^\circ] \\ w_4 = 0,7 \cdot p_w & [120^\circ \div 180^\circ] \end{cases} \quad (12)$$

4.4 Numerical models

The tower has been modeled in a 3D assembly, while both the outer wall and the internal stiffeners are modeled with S4R shell elements as described in the Abaqus Manual (Documentation, Abaqus, and User Manual 2012). For the shell elements, only the conventional shell model geometry is designed and the shell thickness is taken into account by the section properties. These shell elements consist of 4 nodes and they have both translational and rotational degrees of freedom at their nodes. The middle surface is considered to be the reference surface of the shell. The stiffening rings that are introduced in the structure are also modeled with shell elements since their main function is to undertake stresses within their plane. The stiffening rings

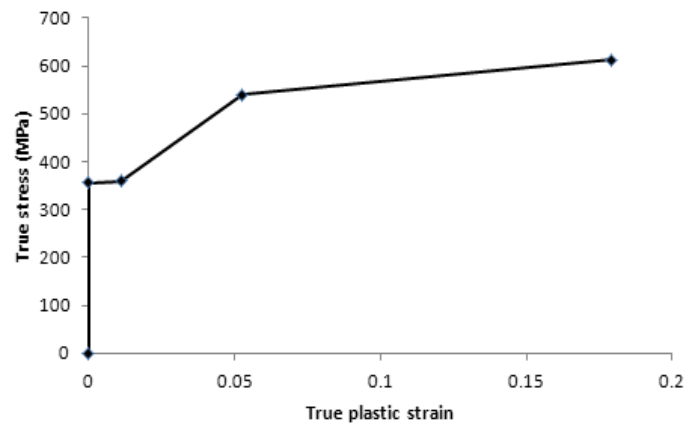


Fig. 5 Material law used in the analyses

that consist of S4R shell elements are positioned transverse to the tower wall as shown in Fig.1 and again their thickness is taken into account by the section properties. The thickness of the rings is greater than the tower's shell. The thickness of the stiffening rings is considered as 22 mm, their width is 20 cm and their number is a matter of investigation in this current study. The advantage of modelling internal stiffeners with shell elements is that both in-plane and out-of-plane buckling of the stiffeners can be observed. The stringer stiffeners introduced in the structure are also modeled with shell elements and are positioned vertically to the tower diameter and transverse to the tower wall as shown in detail in Fig. 2. The thickness of the longitudinal stiffeners is 20 mm, their width is 20 cm and their number is a matter of investigation of the present work. The dimensions of the rings and stringer stiffeners are calculated according to the Eurocode provisions. The flanges connecting the consecutive tubular parts are present from the initial model since their presence is imposed by element transportation restrictions. These flanges are 60 mm thick on each part, therefore 120 mm as a total as shown in Fig. 1. Their function is similar to the one of the internal stiffening rings and therefore they contribute to the eigenmode shape of the structure. The stiffeners are normal to the direction of the tower shell; their outer nodes are merged with the inner nodes of the tower wall at certain positions. The meshing of the stiffening schemes and the tower is structured, so that is consistent in the contact area of the two geometries and there is a constant flow between the stresses of different parts.

The steel grade is S355 and the material law introduced is taking into account hardening when going from the yielding stress to the ultimate stress in three branches. The first is an almost constant plateau until 0.011 true strain, the second is a steep branch until 0.0528 true strain and 539 MPa true stress and the third is a smooth branch until ultimate plastic strain 0.174% and ultimate true stress 612 MPa. The material law introduced in the analyses performed in this present work is presented in Fig. 5.

4.5 Methods of analysis

The methods applied for the tower analysis are:

- Static material non-linear analysis without imperfections [GMNA] and
- Static Geometrical and Material Non-linear Imperfection Analysis [GMNIA].

For the latter as proposed by Koiter (1945) and Speicher and Saal (1991) the equivalent imperfection introduced in the structure is of the same form as the first bifurcation mode with an adjusted amplitude proposed by the design codes. As a consequence, a bifurcation analysis is first carried out to obtain the buckling shapes of the structure and the eigenvalues necessary for the geometrical and material non-linear imperfection analysis. The eigenvalue analysis is a hint of the theoretical ultimate buckling load of the structure without initial imperfections. The static non-linear analysis is then carried out to show the response of the tower again without initial imperfections.

4.6 Stiffening schemes

Along with the unstiffened tower which is analyzed for the purposes of comparison, five different types of tower models are used with different number of stiffening rings introduced at the tower shell as shown in Figs. 6 and 7. In addition four different models are investigated with different number of longitudinal stringer stiffeners introduced at the tower shell as shown in Fig. 8. In total the analyzed models are:

- the unstiffened original tower [US],
- a tower model including 3 stiffening rings, one at each tower part [3R],
- a tower model including 9 stiffening rings, 3 at each tower part [9R],
- a tower model including 15 stiffening rings, 5 at each tower part [15R],
- a tower model including 21 stiffening rings, 7 at each tower part [21R].
- a tower model including 1 longitudinal stiffener [1V],
- a tower model including 2 longitudinal stiffeners [2V],
- a tower model including 3 longitudinal stiffeners [3V],
- a tower model including 4 longitudinal stiffeners [4V].

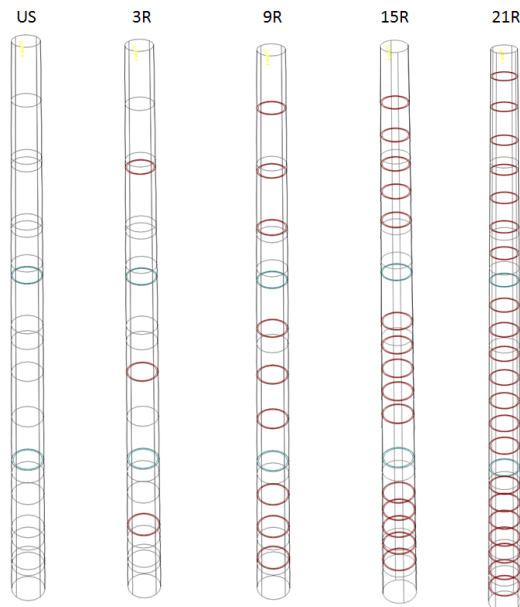


Fig. 6 Structural models analyzed, including unstiffened tower and four different stiffening schemes

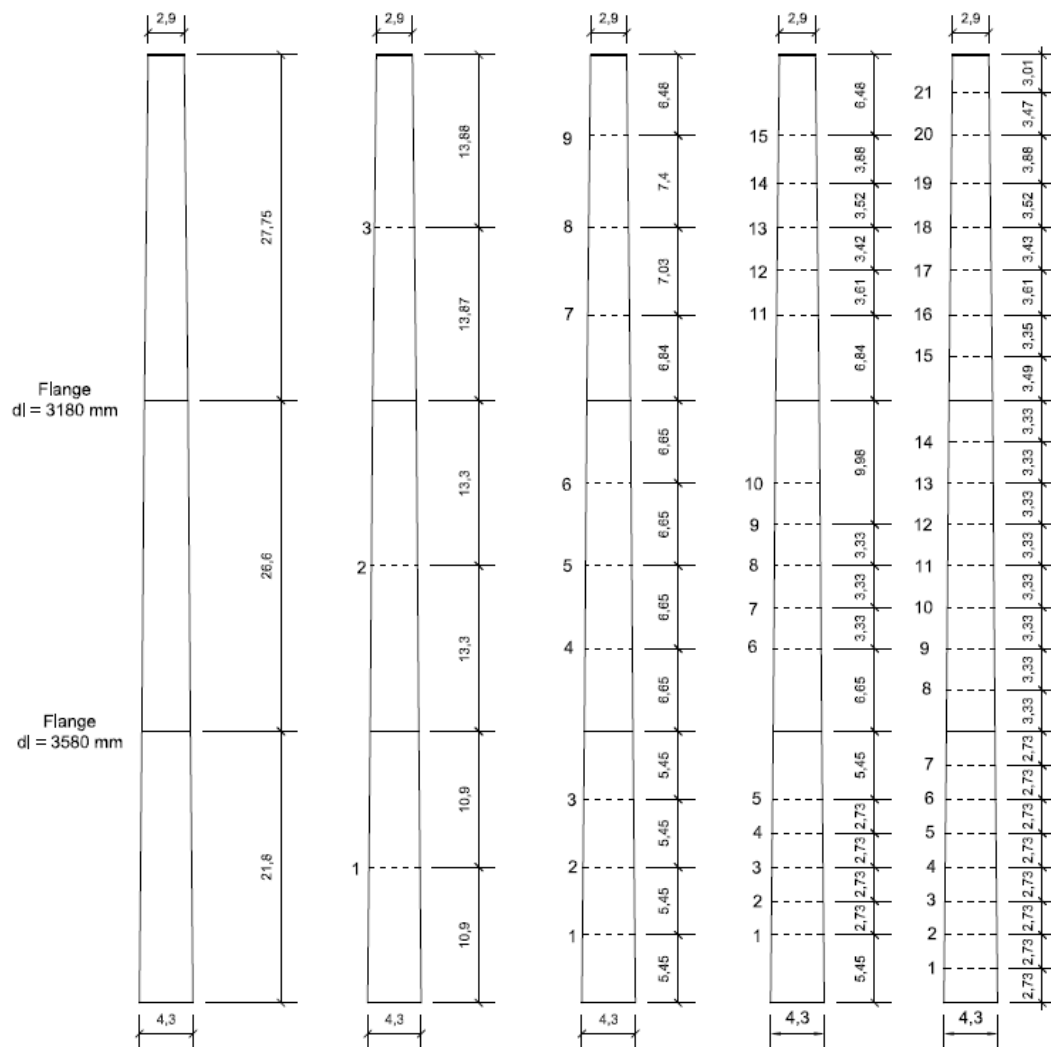


Fig. 7 Details, dimensions and spacing of stiffening rings in the different configurations

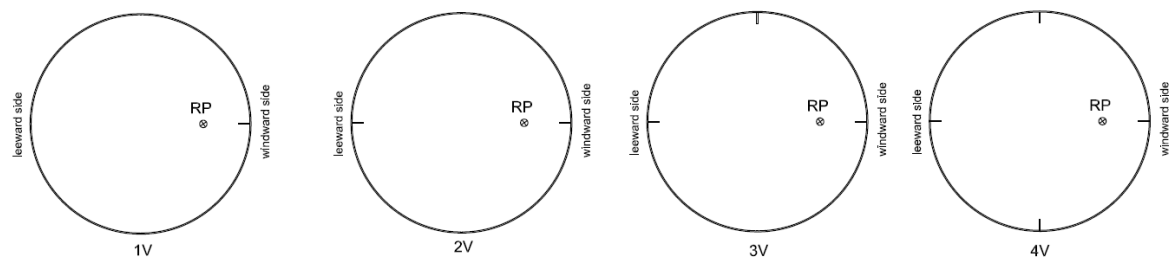


Fig. 8 Longitudinal stiffeners configurations

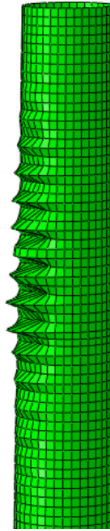


Fig. 9 Compression buckling shape of first Eigenmode of US

5. Results for the unstiffened tower

5.1 Eigenvalue analysis

An initial bifurcation analysis is imperative for the calculation of the critical buckling load of the structure and the calculation of the eigenmode shapes of the structure that can be introduced with the use of certain amplitude as the initial imperfections of the structure. In order to conduct an initial calculation, a linear buckling analysis is performed separately to show the influenced region. The first eigenmode is shown in Fig. 9 where the compressive short wavelength buckling shape is dominant. This buckling shape is characteristic of the presence of bending moment or compressive forces.

5.2 GMNA and GMNIA analysis of the unstiffened tower

After having performed the eigenvalue analysis the deformed shape of the 1st eigenmode is used with the relevant amplification factor as the initial imperfections of the tower. The introduction of initial imperfections is performed by using the deformed shape of the first eigenmode multiplied by an amplification factor proposed by the Eurocode, (EN 1993-1-6 2006) and evidently both [GMNA] and [GMNIA] analyses are performed. Taking into account the initial imperfections of the tower, which in this case are short wavelength buckling shapes of the first eigenmode are initializing more complicated deformations like “ovalization” of the cross-section and long wavelength buckling shapes of the circumference of the shell. This is proved by the fact that these more complicated deformations are only observed when performing geometrically and material non-linear imperfection analysis and not simple geometrical and material non-linear analysis. For both methods of analysis a concentration of high von Mises stresses appears close to the top part of the structure as shown in Fig. 10. When the tower buckles, the von Mises stresses have passed beyond the yielding point and the deformed shape indicates the presence of buckling failure. For the [GMNA] case, no such failure type is present, which indicates the immense

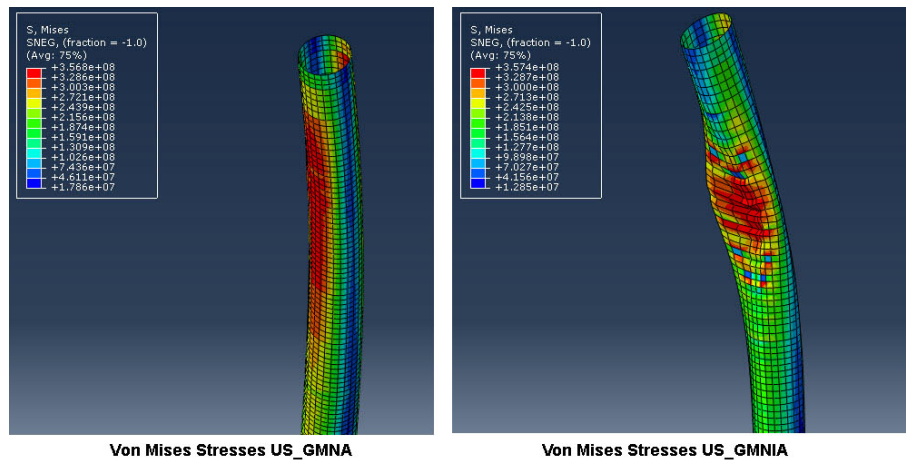


Fig. 10 Von Mises stresses for [MNA] and [GMNIA] for the US model

importance of imperfections to the final failure of the structure.

The response of structure is described in Fig. 11. The vertical axis represents the load factor which is applied on the structure and the horizontal axis represents the horizontal displacement of the top of the tower. The dashed line represents the material non-linear analysis of the tower [GMNA] and the solid line represents the material nonlinear imperfection analysis of the tower [GMNIA]. The load where the structure fails without the introduction of the initial imperfections is about 0,6 P and the one with the introduction of the initial imperfections is about 0,44 P. This is about one fourth of the load indicated by the eigenvalue analysis. This phenomenon of shells that buckle at a lower ultimate load than the one that is shown by the eigenvalue analysis is expected and has been described extensively in the cylindrical shells theory. The problem that is under investigation is a bending dominated problems where there is a strong presence of short-wavelength buckles. The introduction of stiffeners, both vertical and horizontal, is attempted. The influence of ring stiffeners is expected to limit to some extent the phenomenon of ovalization of the cross-section, while the vertical stiffeners are expected to limit the presence of the short-wavelength buckles.

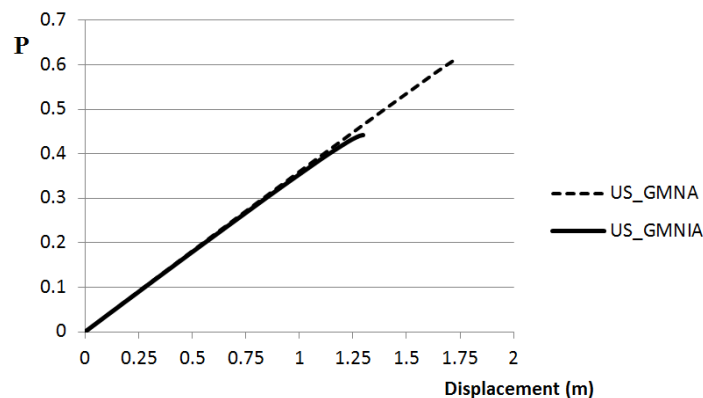


Fig. 11 Comparison of [GMNA] and [GMNIA] analyses of the unstiffened structure US

6. Results for the different stiffening schemes

6.1 Eigenvalue analysis

For all the analyzed schemes, both stiffened and unstiffened, the mesh of the models is maintained almost the same in order to avoid any numerical incoherence. The unstiffened structure has just the two stiffening rings at the connections between consequent parts of the structure and the stiffened structures include the internal rings and the longitudinal stiffeners respectively. The stiffening rings are added at equal distances in between each part as shown in Figs. 6 and 7 while the longitudinal stiffeners are positioned symmetrically around the circumference of the shell dividing it into 4 equal parts.

As it can be derived from Table 1 the introduction of the stiffeners improves the behavior of the tower. This is reflected to the critical buckling load calculated for all the cases. The more stiffeners added to the cylinder the higher the critical buckling load. After conducting a linear perturbation analysis for each model, the non-linear imperfection analysis that follows, is performed using as initial imperfections, the 1st eigenmode shape of the relevant structure with the appropriate imperfection factor.

6.2 Ring stiffened structures [GMNA] analysis

The static nonlinear analysis without imperfections, shows that the response of the stiffened structures is better than the unstiffened one. The ultimate load that the stiffened structure can sustain can be seen from Fig. 16. The ultimate load for the tower with 3 rings is 0,64P, for the tower with 9 rings is 0,65P, for the tower with 15 rings is 0,67P and for the tower with 21 rings is 0,69P. In Figs. 12-13 the Von Mises stresses of the structure are shown. The area around the stiffening rings is relieved in the structures that have denser ring schemes while in the unstiffened structure and the 3R case, the stresses are distributed in a wider area with greater values. This relief in the shell stresses can be observed better in the structures where rings are added closer to

Table 1 Eigenvalues of stiffened and unstiffened towers

	1 st Eigenvalue	2 nd Eigenvalue	3 rd Eigenvalue	Difference of 1 st Eigenvalue
US	2.0056	2.0229	2.2348	-
3R	2.0326	2.1293	2.3489	1.35%
9R	2.0814	2.2098	2.3381	3.5%
15R	2.3316	2.4905	2.7459	16.58%
21R	2.3832	2.5828	2.7879	18.83%
1V	2.0801	2.1111	2.3324	4.00%
2V	2.2029	2.2068	2.2070	9.83%
3V	2.7740	2.8390	2.8575	38.3%
4V	2.7790	2.8416	2.8637	38.56%

*US: Unstiffened Structure; 3R: Stiffened structure with 3 rings; 9R: Stiffened structure with 9 rings; 15R: Stiffened structure with 15 rings; 21R: Stiffened structure with 21 rings; 1V: Stiffened structure with 1 stringer stiffener, 2V: Stiffened structure with 2 stringer stiffeners, 3V: Stiffened structure with 3 stringer stiffeners, 4V: Stiffened structure with 4 stringer stiffeners

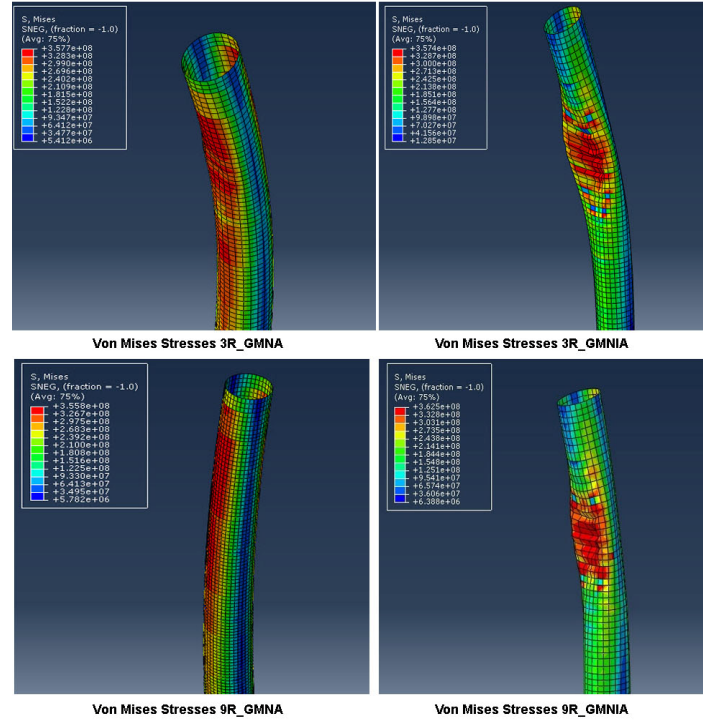


Fig. 12 Von Mises stresses for [GMNA] and [GMNIA] for the models 3R and 9R

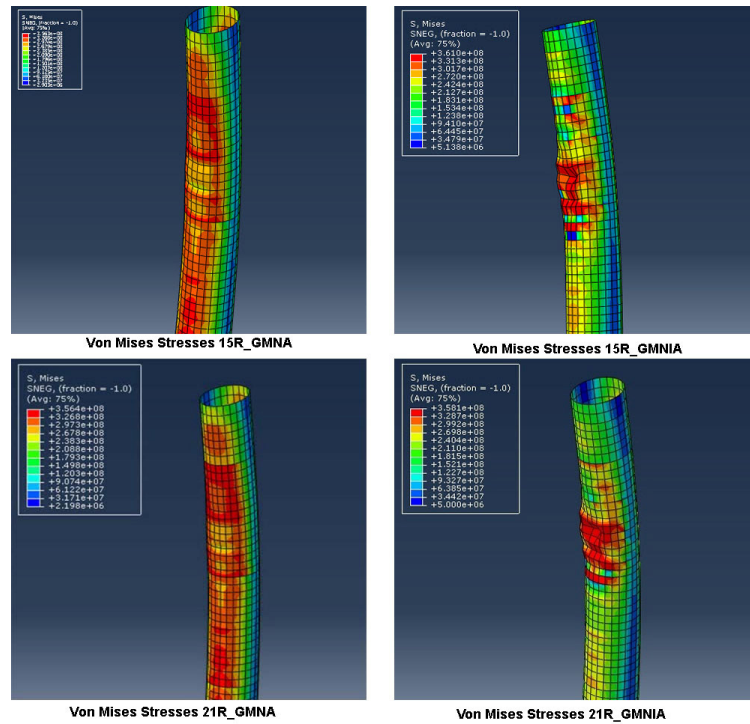


Fig. 13 Von Mises stresses for [GMNA] and [GMNIA] for the models 15R and 21R

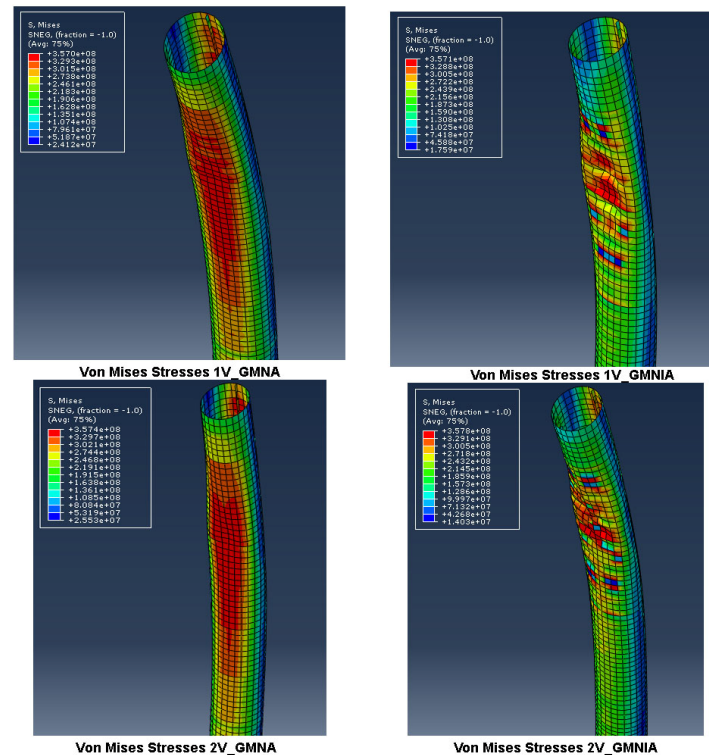


Fig. 14 Von Mises stresses for [GMNA] and [GMNIA] for the models 1V and 2V

the area where buckling is occurring. The increase of the capacity of the structure is slightly higher between the 9R and 15R structures reflecting the difference of adding the rings in the mostly influenced area.

6.3 Stringer stiffened structures [GMNA] analysis

The static nonlinear analysis without imperfections, shows that the response of the longitudinally stiffened structures is better than the unstiffened one. The ultimate load that these stringer stiffened structures can sustain can be observed in the diagrams presented in Fig. 17. The ultimate load for the tower with 1 stringer stiffener is 0,64P, for the tower with 2 stringer stiffeners is 0,69P, for the tower with 3 stringer stiffeners is 0,693P and for the tower with 4 stringer stiffeners is 0,694P. In Figs. 14-15 the Von Mises stresses of the structures are presented. The influenced area more likely to fail is located at the upper one third of the tower with the von Mises stresses exceeding the yielding point of the material. A slight “ovalization” of the tower shell is observed in all the cases showing that stringer stiffeners do not function against this phenomenon. The increase of the capacity of the structure is slightly higher between the 1V and 2V structures compared to the increase between 2V-3V and 3V-4V showing that the two stiffeners vertically to the moment and shear load are the ones that function better against bending. The first two longitudinal stiffeners implemented in the model are positioned accordingly in order to withstand the bending and shear load. The eigenvalue of the structure 2V has a significant difference compared to the unstiffened one. The next two longitudinal stiffeners placed at the positions specified in Fig. 8 are mainly

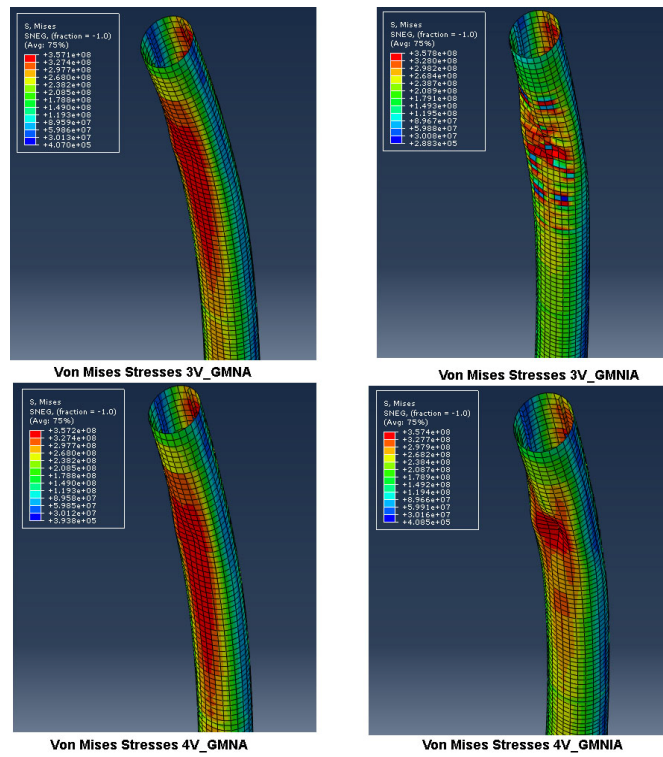


Fig. 15 Von Mises stresses for [GMNA] and [GMNIA] for the models 3V and 4V

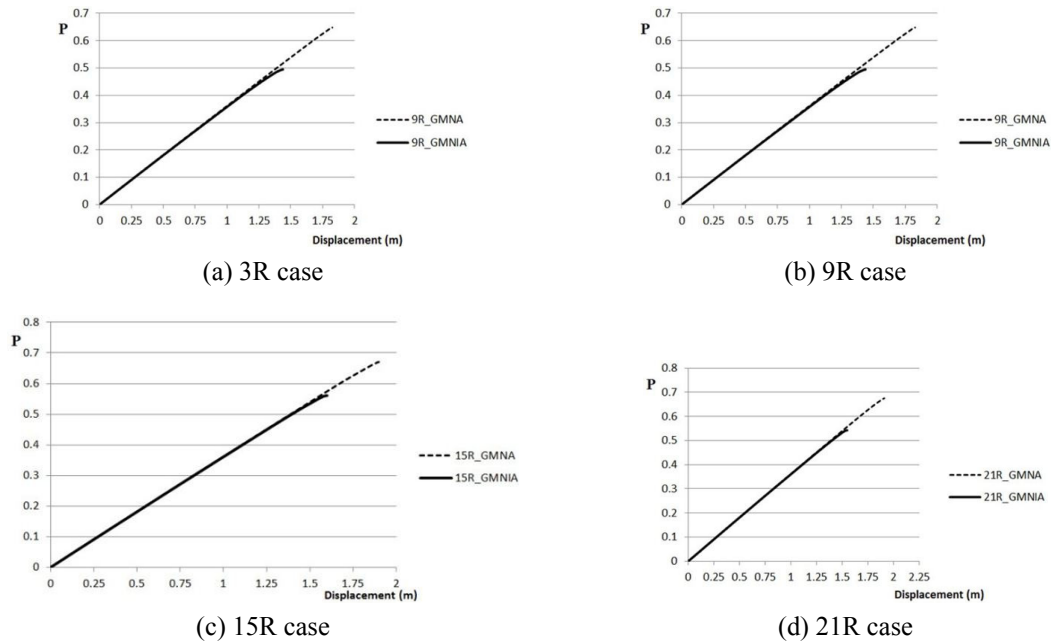


Fig. 16 Comparison of [GMNA] and [GMNIA] analyses of all the ring stiffened schemes

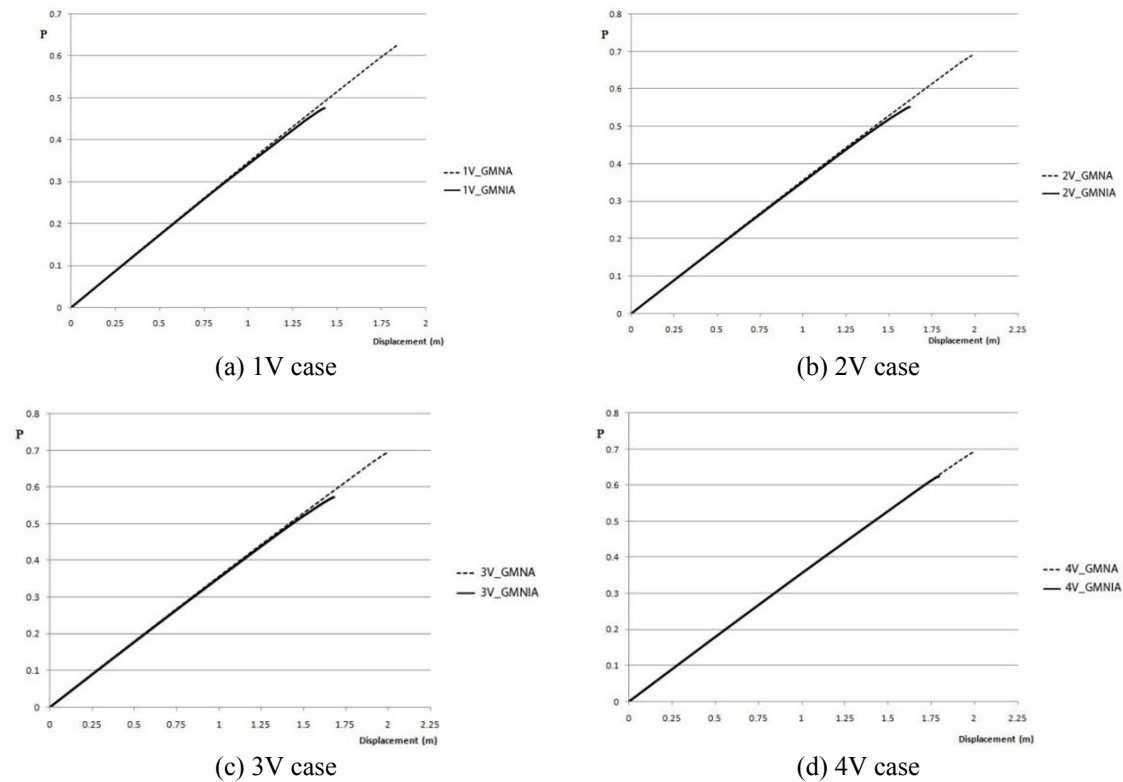


Fig. 17 Comparison of [GMNA] and [GMNIA] analyses of all the stringer stiffened schemes

placed for symmetry and their inertia does not influence much the bending and shear capacity of the structure, which is reflected in the minor difference between the eigenvalue of model 4V and US.

6.4 Ring stiffened structures [GMNIA] analysis

With the introduction of the initial imperfections to the structural analysis the ultimate load is dropping for all the models, both stiffened and unstiffened. It is characteristic that for the ring-stiffened models, GMNIA results appear to be 15% lower respectively to the GMNA ones for all models 3R to 21R. This reflects the great degree of sensitivity of shell structures to initial imperfections. Fig. 16 shows that the ultimate buckling load of 3R is 0,47P, of 9R is 0,49P, of 15R is 0,56P and of 21R is 0,57P. For [GMNIA], the difference in the response of the towers is greater than before. It is remarked that for the ring-stiffened structures and especially for the 9R and 15R cases the ultimate buckling load increases about 14%. This reflects the importance of the rings position in the tower response. For the 15R structure there are more rings added to the area that is more vulnerable to buckling and therefore the ultimate load increases remarkably. The most remarkable difference to be observed from the results of the analyses is the difference in the shape of the failure among the models. The first three models US, 3R and 9R have the similarity that in addition to the short wavelength buckles of compressive nature, an ovalization of the tower cross-section is observed in the upper part of the tower. This type of deformation dominated by

long wavelength buckling shapes is mainly controlled by the presence of the stiffening rings. This can be observed in the limiting of ovalization observed between US and 15R models. As extracted from Table 2, the US structure deforms uniformly in the transverse and normal direction. On the contrary the 15R structure has a local deformation on the transverse direction while keeping the circular shape in the normal direction. The effect of the introduction of stiffening rings in the affected area is reflected in the difference of the buckling shape between 9R and 15R models, where rings are added in the area where this “ovalization” occurs. In addition it is also reflected in the great difference in the buckling load between the two models. In the 15R model this phenomenon is eliminated, therefore the further introduction of rings has a limited effect both on the shape and the buckling load, which is seen in 21R model. The presence of ovalization in the

Table 2 Effect of ovalization on the tower shape

	US_GMNIA	15R_GMNIA	4V_GMNIA
Undeformed diameter	3.080	3.056	3.123
Deformed normal distance	3.189	3.068	3.138
Deformed transverse distance	2.912	2.938	3.036

*Deformed normal distance (N) in meters as indicated in Fig. 23, Deformed transverse distance (T) in meters as indicated in Fig. 23

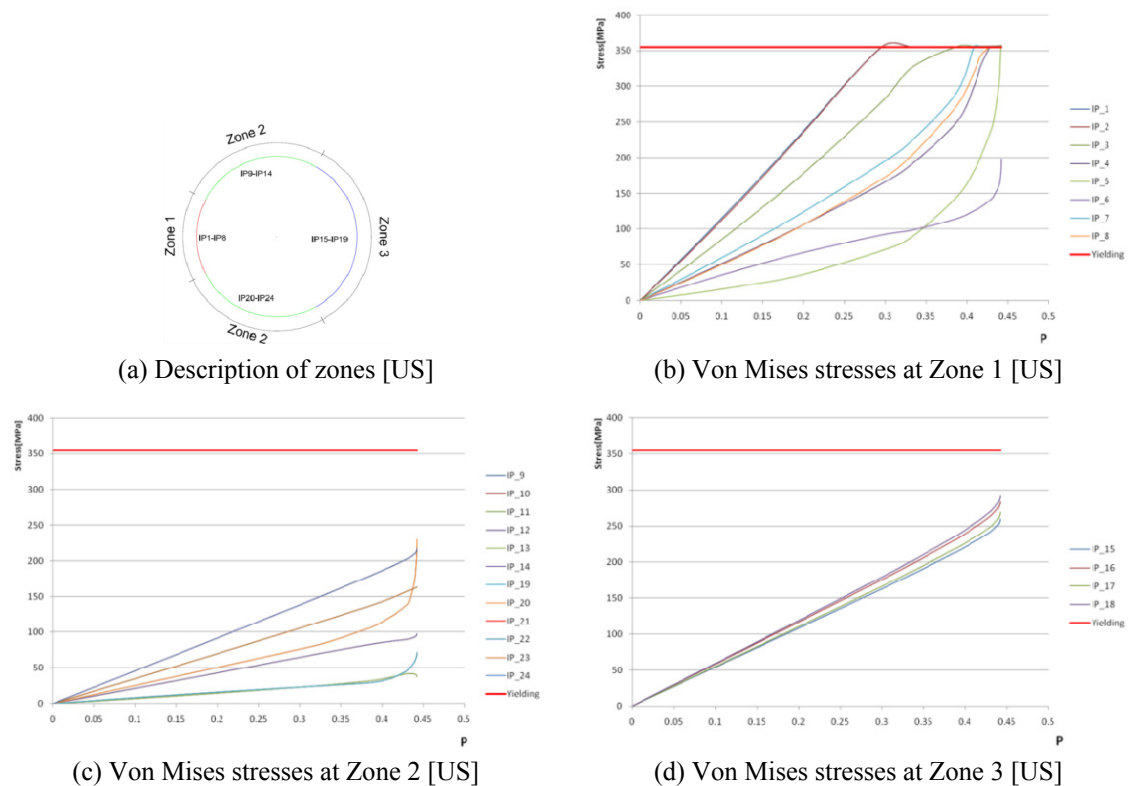


Fig. 18 Von Mises stresses around the circumference for the US model

models US, 4V in contradiction with its absence in the model 15R is reflected in Fig. 23. The bottom diameter illustrated is the one at 10m above the ground which is perfectly circular for all the models; US, 4V and 15R. The top diameter presented is the one at 63m above the ground which is the area most affected by loading and more vulnerable to failure for all the models investigated. In that height it is clear that the US and 4V diameters are “ovalized”, having lost their circular shape, while in the 15R the circular shape is maintained due to the introduction of stiffening rings.

Another observation that can be made is that with the introduction of rings the buckling capacity of the structure is increased and the circumferential stresses are noticeably reduced. The rings function beneficially on the structure in reducing the impact of the initial imperfections which can be seen from the fact that the difference in the ultimate load between US.GMNA and US.GMNIA is 36%, 3R.GMNA and 3R.GMNIA is 36%, 9R.GMNA and 9R.GMNIA is 32%, but for 15R is 20% and for 21R is 19%. Again the greater difference appears between 9R and 15R structures demonstrating the importance of the positioning of the rings. The more rings added closer to the influenced area, the greater the impact that is reflected in the ultimate capacity of the structure. The occurrence of buckling for all the models is presented through the von Mises stresses around the circumference of the shell at the area where failure is occurring displayed in Figs. 18-22. Zone 1 is the leeward side of the tower showing very high stresses forming the potential buckling zone. The sides which are represented in zone 2 have very low stresses and the windward side of the tower has stresses that towards the final load step have higher values but are below yielding.

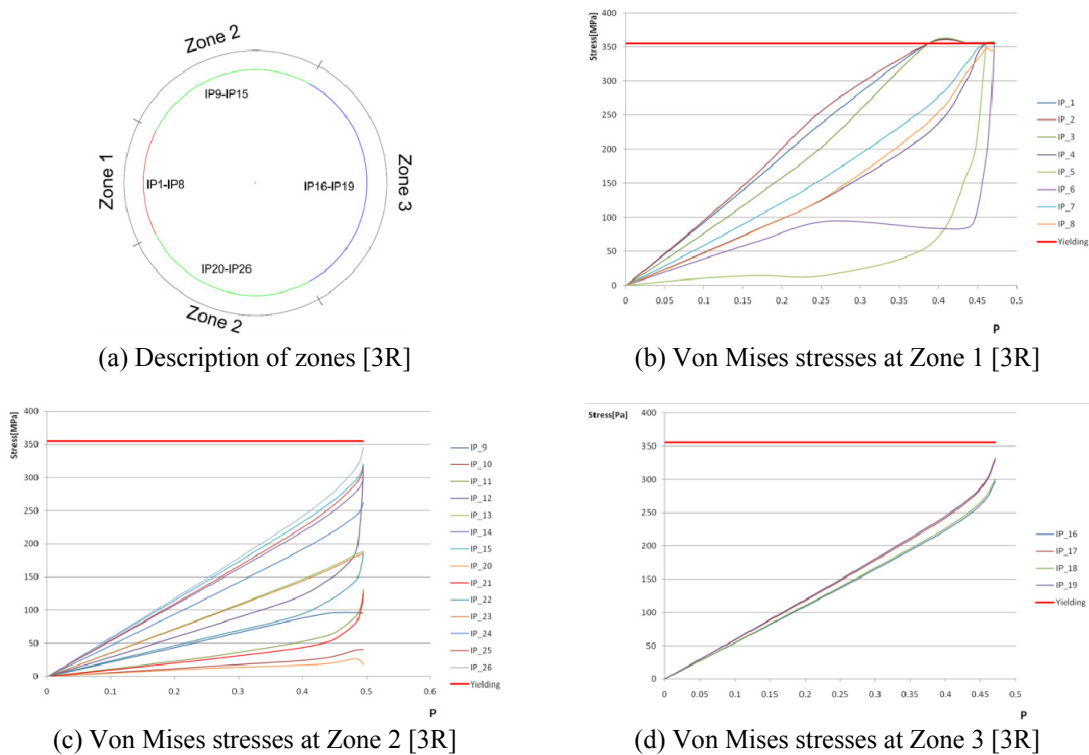


Fig. 19 Von Mises stresses around the circumference for the 3R model

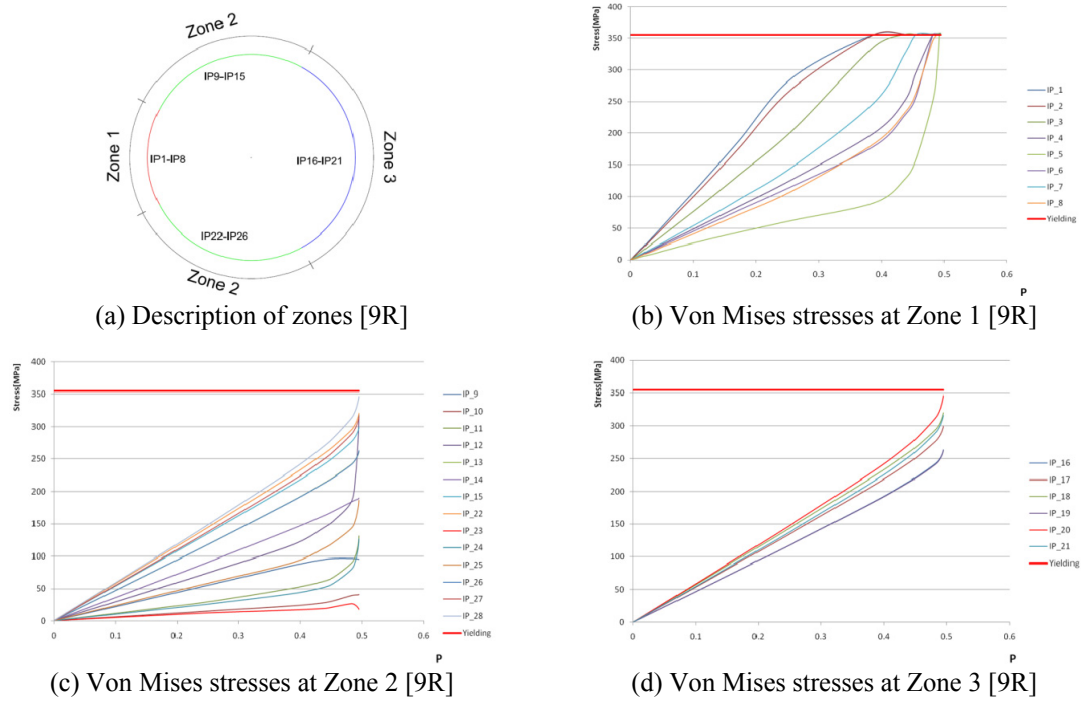


Fig. 20 Von Mises stresses around the circumference for the 9R model

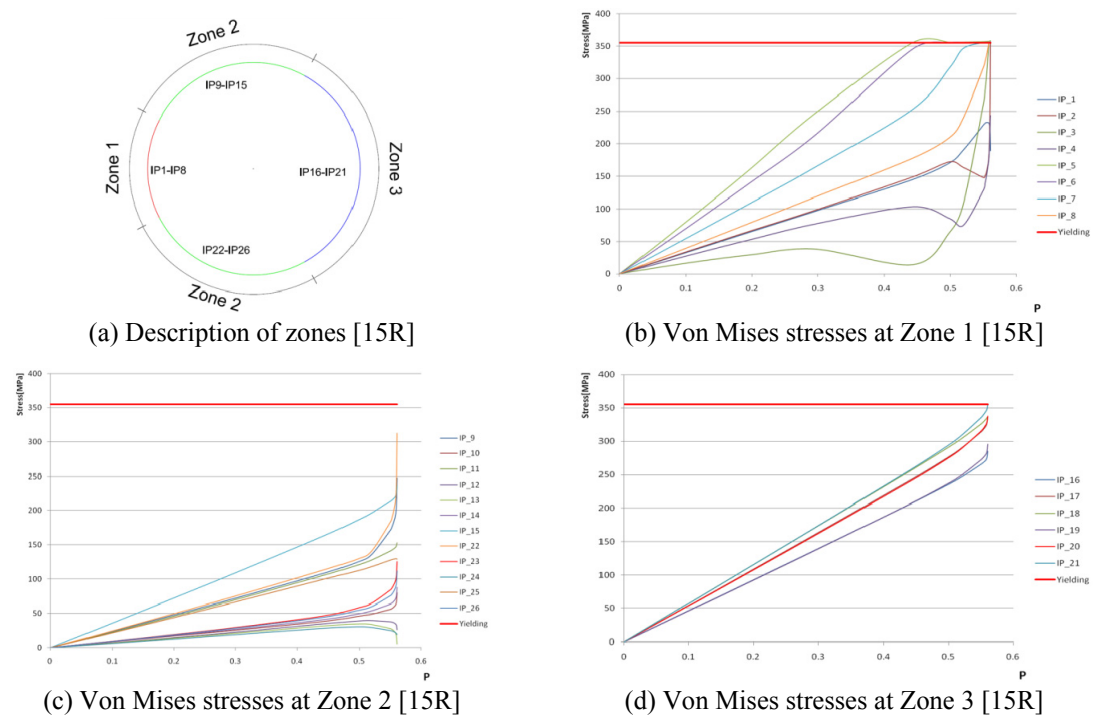


Fig. 21 Von Mises stresses around the circumference for the 15R model

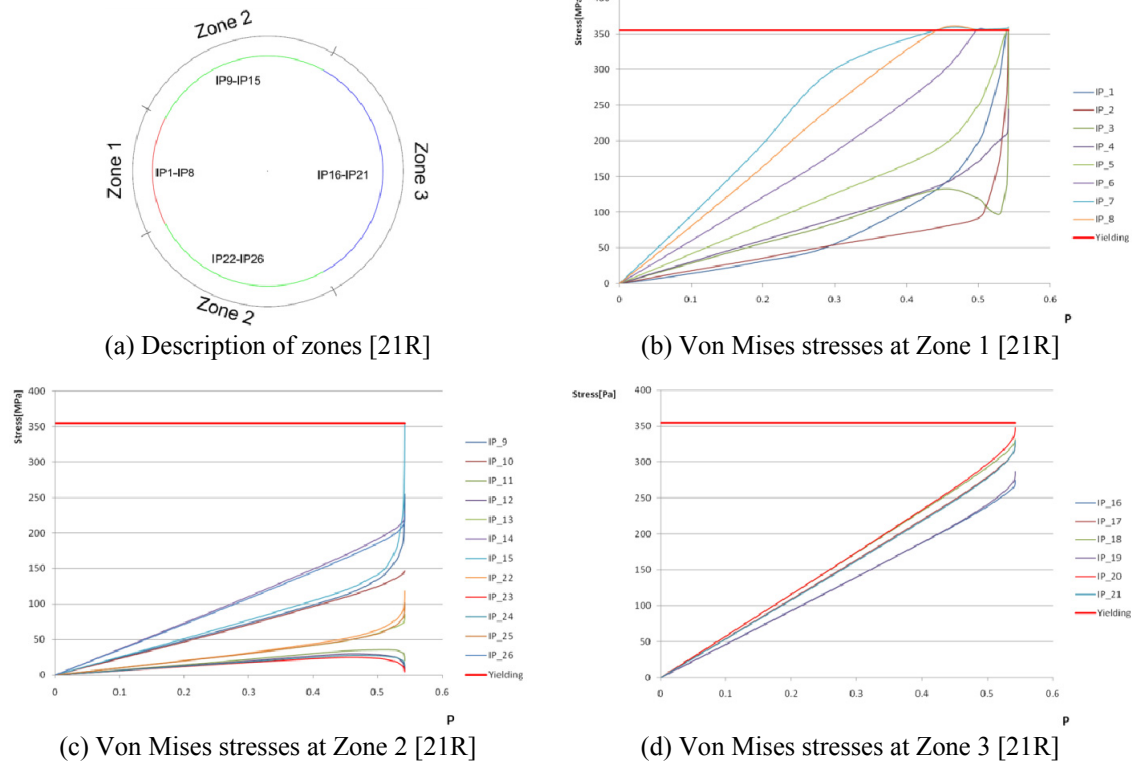


Fig. 22 Von Mises stresses around the circumference for the 21R model

6.5 Stringer stiffened structures [GMNIA] analysis

With the introduction of the initial imperfections to the structural analysis the ultimate load is dropping also for all the stringer-stiffened models about 20%. This highlights the importance of conducting calculations taking into account initial imperfections for complicated structures. Fig. 17 shows that the ultimate buckling load of 1V is $0,48P$, of 2V is $0,55P$, of 3V is $0,57P$ and of 4V is $0,63P$. For [GMNIA], the difference in the response of the towers is greater than before. It is remarked that for the stringer-stiffened structures and especially between 1V and 2V cases the ultimate buckling load increases more than 15%. The importance of placing stringer stiffeners symmetrically is highlighted along with the fact that the stiffeners perpendicular to the shear and bending loads contribute to increasing the buckling capacity of the structure. The presence of ovalization in all the stringer stiffened structures is observed, highlighting the fact that this phenomenon is purely controlled by the introduction of ring-stiffeners. In Table 2 the structure 4V is observed to deform uniformly on the transverse and normal direction, indicating that it is ovalized. This absence of the circular shape is limited compared to the US structure, but the phenomenon is not localized buckling. In all the models, both ring-stiffened and stinger stiffened short wavelength buckling shapes of compressive nature arise in the upper part of the tower. In the models 1V, 2V and 3V these buckling deformations are of shorter wavelength at the circumference of the tower and the longitudinal stiffener is proved to function as a pin end for the tower shell. In the last model, 4V there is an absence of short wavelength buckling deformations and the panel

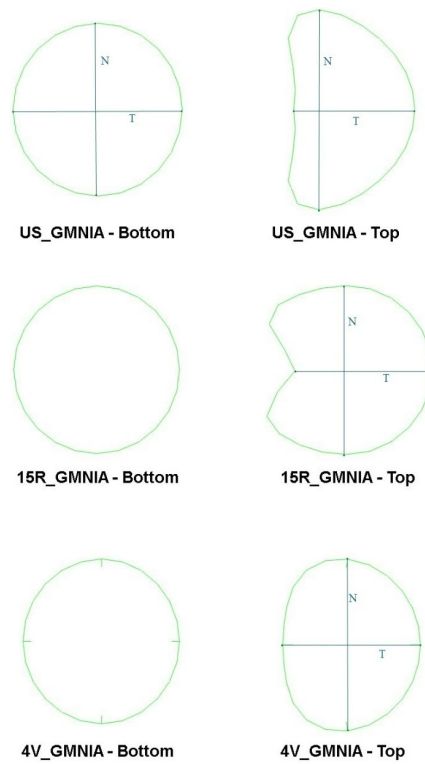


Fig. 23 Deformed cylindrical shape – ovalization phenomenon

buckling mode is proved dominant, indicating that with the use of stiffer longitudinal stiffeners or with denser positioning, short wavelength buckling deformations of compressive nature can be controlled by stringer stiffeners.

Another observation that can be made is that with the introduction of longitudinal stiffeners the buckling capacity of the structure is increased and the impact of the initial imperfections is limited. The latter can be observed from the fact that the difference in the ultimate load between 1V.GMNA and 1V.GMNIA is 33%, 2V.GMNA and 2V.GMNIA is 25%, 3V.GMNA and 3V.GMNIA is 21% and for 4V is 10%.

6.6 Stiffening performance index

The introduction of internal stiffeners needs to be investigated in the aspect of the capacity gain counterbalanced by the additional weight added to the structure. The concept of internal stiffening of wind turbine towers is based on the idea of adding elements with high stiffness/weight ratio in critical positions so that the capacity of the structure is maximized while the weight of the structure is slightly increased. A new stiffening performance index is defined, which takes into account the added weight of the structure along with the respective increased capacity as indicated in Eq. (13) as follows

$$I = \frac{C' - C}{C * W} \quad (13)$$

Table 3 Capacity index over the tower weight

	W increase (%)	GMNIA Index
US	-	-
3R	0.19	0.0591
9R	0.56	0.0342
15R	0.94	0.0409
21R	1.31	0.0254
1V	0.43	0.0291
2V	0.87	0.0419
3V	1.30	0.0317
4V	1.73	0.0305

*US: Unstiffened Structure; 3R: Stiffened structure with 3 rings; 9R: Stiffened structure with 9 rings; 15R: Stiffened structure with 15 rings; 21R: Stiffened structure with 21 rings; 1V: Stiffened structure with 1 stringer stiffener; 2V: Stiffened structure with 2 stringer stiffeners; 3V: Stiffened structure with 3 stringer stiffeners; 4V: Stiffened structure with 4 stringer stiffeners

Where C' is the capacity of the stiffened structure, C is the capacity of the unstiffened structure and W is the weight due to the stiffening scheme under examination. The results of the calculation of the above described index are presented in Table 3.

As already discussed above, the introduction of stiffeners is proved to be more beneficial when conducting analyses with introduction of initial imperfections. The stiffeners limit phenomena deriving from these prebuckling deformations and increase the capacity of the structure. The increase in the weight of the structure is trivial compared to the gain in the capacity which is proved by the fact that the stiffeners do not constitute more than 1,7% of the weight of the

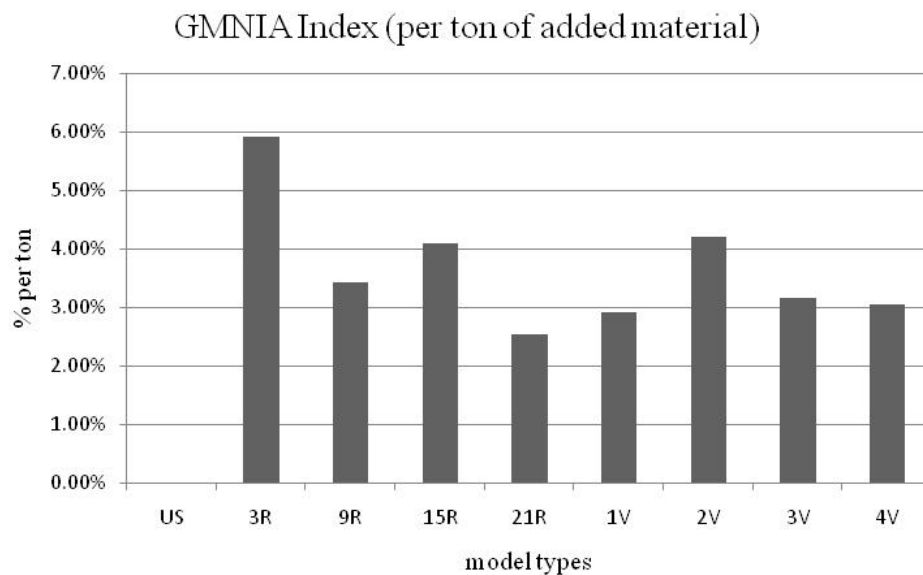


Fig. 24 GMNIA Index per ton of added material to the structure

structure even in the most heavily stiffened cases, while the gain in capacity is in some cases over 30% compared to the unstiffened structure.

7. Conclusions

The focus of the present work is put on the investigation of the function of internal stiffening of wind turbine towers towards buckling phenomena. The analysis of both the unstiffened tower and various schemes of stiffened structures with material nonlinear analysis and material nonlinear analysis with initial imperfections shows the great sensitivity of wind turbine towers to initial imperfections added to the structure. As expected, the more stiffeners are added to the structure the greater is the ultimate capacity of the structure in both cases of perfect and imperfect structures. The differences between the unstiffened and the stiffened structures are much greater in the material nonlinear imperfection analyses which reflect the beneficial impact of internal stiffening in limiting the effect of the initial imperfections induced in the structure. The rings are responsible for limiting the possible ovalization of the structure and constitute an effective mean especially against external wind pressure. Longitudinal stiffeners on the other part are responsible for limiting deformations induced by bending and shear forces and their beneficial impact is reflected in the increase of the failure load of the stringer stiffened structures. Finally, the positioning of rings proves to be important as the ultimate capacity of the structure with imperfections is much closer to the ultimate capacity without imperfections to the models where stiffening rings are implemented in the area where failure is most likely to occur. The presence of the short wavelength buckling deformations is mainly controlled by the presence of vertical stiffeners. In the model with four symmetrically positioned longitudinal stiffeners the results of GMNA and GMNIA analyses are very close indicating the beneficial function of stringer stiffeners in limiting the effect of initial imperfections. In wind turbine towers the use of orthogonally placed stiffeners, which is the combination of longitudinal and ring stiffeners, is effectively limiting the deformations induced by the combination of wind pressure and shear and bending forces and their optimal distribution is the aim of future work.

Acknowledgments

The first author wants to express her gratitude to IKY for financial support of the research activities on performing her PhD thesis through the IKY Fellowship of Excellence for Postgraduate Studies in Greece – SIEMENS Program

This research has been co-financed by the European Union (European Social Fund-ESF) and Greek national funds through the Operational Program “Education and Lifelong Learning” of the National Strategic Reference Framework (NSRF) - Research Funding Program: THALES: Reinforcement of the interdisciplinary and/or inter-institutional research and innovation.

References

- Arani, A.G., Loghman, A., Barzoki, A.M. and Kolahchi, R. (2010), “Elastic buckling analysis of ring and stringer-stiffened cylindrical shells under general pressure and axial compression via the Ritz method”, *J. Solid Mech.*, **2**(4), 332-347.
- Arasu, P., Sagayaraj, D. and Gowrishankar, J. (2011), “Seismic analysis of a wind turbine steel tower”,

- Proceedings of the HyperWorks Technology Conference*, Pune, India, August.
- Bazant, Z. and Cedolin, L. (2010), *Stability of Structures. Elastic, Inelastic, Fracture and Damage Theories*, World Scientific, Singapore.
- Bazeos, N., Hatzigeorgiou, G., Hondros, I., Karamaneas, H., Karabalis D.L. and Beskos, D. (2002), "Static, seismic and stability analyses of a prototype wind turbine steel tower", *Eng. Struct.*, **24**(8), 1015-1025.
- Bushnell, D. (1976), "Buckling of elastic-plastic shells of revolution with discrete elastic-plastic ring stiffeners", *Int. J. Solids Struct.*, **12**(1), 51-66.
- Calladine, C. (1989), *Theory of Shell Structures*, Cambridge University Press, Cambridge, England.
- Chen, L. and Rotter, J.M. (2012), "Buckling of anchored cylindrical shells of uniform thickness under wind load", *Eng. Struct.*, **41**, 199-208.
- Chen, L., Doerich, C. and Rotter, J.M. (2008), "A study of cylindrical shells under global bending in the elastic-plastic range", *Steel Construct.*, **1**(1), 59-65.
- Chen, L., Rotter, J.M. and Doerich, C. (2011), "Buckling of cylindrical shells with stepwise variable thickness under uniform external pressure", *Eng. Struct.*, **33**(12), 3570-3578.
- Dimopoulos, C. and Gantes, C. (2012), "Experimental investigation of buckling of wind turbine tower cylindrical shells with opening and stiffening under bending", *Thin-Wall. Struct.*, **54**, 140-155.
- Dimopoulos, C. and Gantes, C. (2013), "Comparison of stiffening types of the cutout in tubular wind turbine towers", *J. Construct. Steel Research*, **83**, 62-74.
- DNV-RP-C202 (2013), Buckling Strength of Shells, DNV-GL.
- Documentation, Abaqus, and User Manual (2012), Version 6.12, Simulia, DassaultSystèmes.
- European Convention for Constructional Steelwork (2008), *Buckling of Steel Shells: European Recommendations*, ECCS Publications; Brussels, Belgium.
- EN 1991-01-01 (2005), Eurocode 1: Actions on structures: Part 1-4: General actions-Wind actions, CEN.
- EN 1993-01-06 (2006), Eurocode 3: Design of Steel Structures: Part1-6: General Strength and Stability of Shell Structures, CEN.
- EN 1993-03-02 (2006), Eurocode 3: Design of Steel Structures: Part3-2: Towers, masts and chimneys-Chimneys, CEN.
- Flügge, W. (1932), "Die stabilität der kreiszylinderschale", *Ing. Arch.*, **5**, 463-506.
- Galambos, T. (1998), *Guide to Stability Design Criteria for Metal Structures*, John Wiley & Sons, NJ, USA.
- Jansseune, A., De Corte, W., Vanlaere, W. and Van Impe, R. (2012), "Influence of the cylinder height on the elasto-plastic failure of locally supported cylinders", *Steel Compos. Struct., Int. J.*, **12**(4), 291-302.
- Koiter, W.T. (1945), "On the Stability of Elastic Equilibrium", Ph.D. Dissertation; Delft University, Delft, The Netherlands. [In Dutch]
- Lavassas, I., Nikolaidis, G., Zervas, P., Efthimiou, E., Doudoumis, I. and Baniotopoulos, C.C. (2003), "Analysis and design of the prototype of a steel 1-MW wind turbine tower", *Eng. Struct.*, **25**(8), 1097-1106.
- Lee, K. and Bang, H. (2013), "A study on the prediction of lateral buckling load for wind turbine tower structures", *Int. J. Prec. Eng. Manuf.*, **13**(10), 1829-1836.
- Lemak, D. and Studnicka, J. (2005), "Influence of ring stiffeners on a steel cylindrical shell", *J. Adv. Eng. – Acta Polytechnica*, **45**(1), 56-63.
- Lundquist, E. (1933), "Strength tests of thin-walled duralumin cylinders in pure bending", *Tech. Rep.*, National Advisory Committee for Aeronautics, NACA-TN-479, USA.
- Negm, H. and Maalawi, K. (2000), "Structural design optimization of wind turbine towers", *Comp. Struct.*, **74**(6), 649-666.
- Nuta, E., Christopoulos, C. and Packer, J. (2011), "Methodology for seismic risk assessment for tubular steel wind turbine towers: application to Canadian seismic environment", *Can. J. Civ. Eng.*, **38**(3), 293-304.
- Ohga, M., Wijenayaka, A.S. and Croll, J.G.A. (2005), "Buckling of sandwich cylindrical shells under axial loading", *Steel Compos. Struct., Int. J.*, **5**(1), 1-15.
- Ragheb, M. (2013), "Safety of wind systems", Wind Power Systems Course Material; University of Illinois at Urbana-Champaign, IL, USA.
- Rebelo, C., Veljkovic, M., Matos, R. and Simoes da Silva, L. (2012a), "Structural monitoring of a wind

- turbine steel tower – Part II: monitoring results”, *Wind Struct., Int. J.*, **12**(4), 301-311.
- Rebelo, C., Veljkovic, M., Simoes da Silva, L., Simoes, R. and Henriques, J. (2012b), “Structural monitoring of a wind turbine steel tower – Part I: system description and calibration”, *Wind Struct., Int. J.*, **12**(4), 285-299.
- Rotter, J. (1987), “The buckling and plastic collapse of ring stiffeners at cone/cylinder junctions”, *Proceedings of International Colloquium on Stability of Plate and Shell Structures*, Ghent, Belgium.
- Schneider, W. and Brede, A. (2005), “Consistent equivalent geometric imperfections for the numerical buckling strength verification of cylindrical shells under uniform external pressure”, *Thin-Wall. Struct.*, **43**(2), 175-188.
- Schneider, W. and Zahlten, W. (2004), “Load-bearing behavior and structural analysis of slender ring-stiffened cylindrical shells under quasi-static wind load”, *J. Construct. Steel Res.*, **60**(1), 125-146.
- Singer, J. (2004), “Stiffened cylindrical shells”, In: *Buckling of Thin Metal Shells*, Taylor and Francis, London, England, pp. 286-343.
- Speicher, G. and Saal, H. (1991), “Buckling of shell structures, on land, in the sea, and in the air: 466-475, Numerical calculation of limit loads for shells of revolution with particular regard to the applying equivalent initial imperfection”, Elsevier Applied Science.
- Stathopoulos T. and Baniotopoulos, C.C. (2007), *Wind Effects on Buildings and Design of Wind-Sensitive Structures*, Springer Wien, New York, USA.
- Stavridou, N., Efthymiou, E., Gerasimidis, S. and Baniotopoulos, C. (2013), “Modelling of the structural response of wind energy towers stiffened by internal rings”, *Proceedings of the 10th HSTAM International Congress on Mechanics*, Chania, Greece, June.
- Teng, J. (1996), “Buckling of thin shells: Recent advances and trends”, *App. Mech. Rev.*, **49**(4), 263-274.
- Teng, J. and Rotter, J. (2004), *Buckling of Thin Metal Shells*, Taylor and Francis, London, England.
- Timoshenko, S. and Gere, J. (1961), *Theory of Elastic Stability*, Tata McGraw-Hill Education, Noida, UP, India.
- Uys, P., Farkas, J., Jrmaj, K. and Van Tonder, F. (2007), “Optimisation of a steel tower for a wind turbine structure”, *Eng. Struct.*, **29**(7), 1337-1342.
- Veljkovic, M., Heistermann, C. and Husson, W. (2006), “High-strength tower in steel for wind turbines”, *Tech. Rep.*, Publications Office of the European Union.
- Vinson, J. (1988), *The Behavior of Thin Walled Structures: Beams, Plates, and Shells*, Springer, Dordrecht, The Netherlands.
- Wojcik, M., Iwicki, P. and Tejchman, J. (2011), “3D buckling analysis of a cylindrical metal bin composed of corrugated sheets strengthened by vertical stiffeners”, *Thin-Wall. Struct.*, **49**(8), 947-963.